

A NEW ARCHITECTURE FOR MOBILE RADIO WITH MACROSCOPIC DIVERSITY AND OVERLAPPING CELLS

Stefan Zürbes*, Wolfgang Papen* and Werner Schmidt**

* Aachen Univ. of Technology, Institute for Communication Systems and Data Processing
Templergraben 55, 52056 Aachen, Germany
Phone: +49-241-806964, Fax: +49-241-8888186,
E-Mail: zuerbes@ind.rwth-aachen.de

** Ardkeenagh, Boyle, Co. Roscommon, Rep. Ireland
Phone and Fax: +353-79-62883

Abstract: A new mobile radio cell architecture is presented that reduces interferences, increases system capacity, improves transmission quality and allows uncritical hand-offs. Two main features characterize our proposal: *macroscopic diversity supply* of mobiles by means of three base stations which leads to high carrier-to-interference ratios and link quality improvement, and *overlapping cells*, thereby introducing large handoff zones. This system is ideally suited for existing GSM-style digital cellular networks and allows a traffic capacity increase due to a frequency re-use factor of 3.

I. INTRODUCTION

At present, cellular TDMA/FDMA mobile networks are fastly growing in many countries. In Europe, the GSM system (including DCS-1800 in the near future) plays a key role among available mobile communication systems. To obtain high spectrum efficiency and system capacity, the frequency re-use concept is applied [2].

In the past, mostly architectures with one single base station site per cell have found applications, not allowing very small re-use factors. Recently, a new architecture with multiple base stations per cell was presented [5] which allows a cell re-use factor of 3 for the North American AMPS system. It does not contain simultaneous transmission from all base stations nor extensive overlapping of neighboring cells.

The first part of this contribution describes our new cell architecture in relation to conventional ones. Detailed analysis of its quality improvement compared to conventional systems follows, combined with an investigation of new handoff characteristics and considerations of propagation delays.

II. CONVENTIONAL CELL ARCHITECTURES

Fig. 1 shows the well-known cell architecture with a frequency re-use factor of 7 which is denoted as $\langle 7 \rangle$ in the sequel. Omnidirectional antennas are used. Using antenna sectorization leads to a

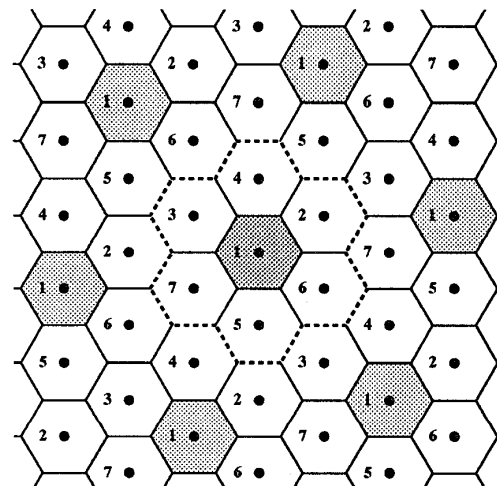


FIG. 1: Conventional non-sectorized cell architecture using 7 frequency groups ($\langle 7 \rangle$)

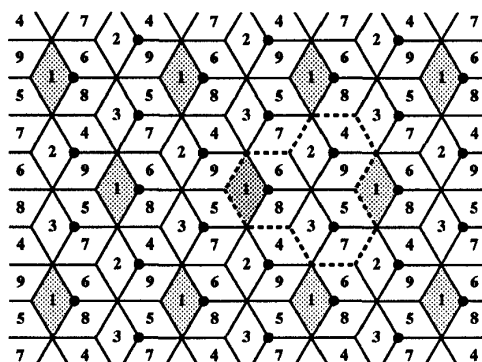


FIG. 2: Conventional sectorized cell architecture using 3 · 3 frequency groups (<3×3>)

more efficient spectrum utilization. The frequency re-use factor is smaller and therefore the number of mobile stations linked to a base station site can be increased. Two different sectorized cell architectures are considered, one requiring 3 · 4 frequency groups (denoted <3×4>) and the other only 3 · 3 groups (denoted <3×3>). A layout of the latter is shown in Fig. 2. Due to smaller distances between cochannel cells, the obtained cochannel carrier-to-interference ratio is lower for the <3×3> cluster. The handoff areas between sectors of the same base station are determined by the antenna characteristic and usually are very small, implying a relatively high probability of losing a connection during handoff. The main characteristics concerning spectrum and user capacity are listed in Table 1 in the next section.

III. NEW CELL ARCHITECTURE

The new cell architecture under consideration is presented in Fig. 3. Its main features are *macroscopic diversity supply* of the mobile station by three base stations and *overlapping cells*, so that each point in the plane belongs to two cells. As shown, this architecture represents a double 3-cell cluster. This structure of six overlapping cells can be repeated periodically in the plane.

Each cell is supplied by three base stations located at every other edge of the cell hexagon; accordingly, each base station site requires six antennas with 120° sectorized characteristics. Only

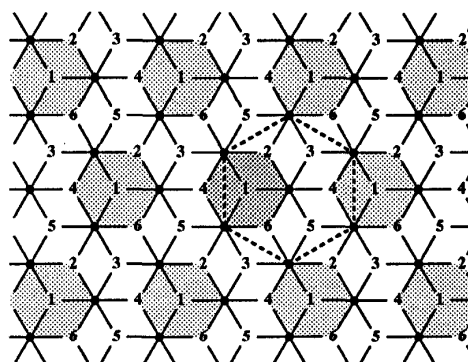


FIG. 3: New architecture with 2 · 3 frequency groups (<2×3>)

six different frequencies or frequency groups are necessary to realize this configuration within the whole plane. The additional implementation complexity for an existing network is moderate, since no additional base station sites are needed.

The resulting user and spectrum capacities are compared to the conventional clusters in Table 1. The first row lists the user capacities per area ρ_A

TABLE 1
Capacity characteristics

	architecture			
	<2×3>	<7>	<3×4>	<3×3>
ρ_A	$\frac{K}{3A}$	$\frac{K}{7A}$	$\frac{K}{4A}$	$\frac{K}{3A}$
ρ_m	$\frac{K}{3}$	$\frac{K}{7}$	$\frac{K}{12}$	$\frac{K}{9}$

for the different architectures, where K denotes the number of totally available traffic channels and A the area of a hexagonal cell. The new cell architecture obtains the same capacity as the <3×3> cluster. The second row shows the maximum number of traffic channels ρ_m at a single location. Since the new architecture combines large cell areas with a multiple supply due to overlapping, it is able to cope with local user concentrations much better than conventional architectures.

IV. CARRIER-TO-INTERFERENCE RATIOS

As a first figure of merit, the resulting minimum carrier-to-interferer (C/I) power ratios for the considered architectures were calculated, ignoring fad-

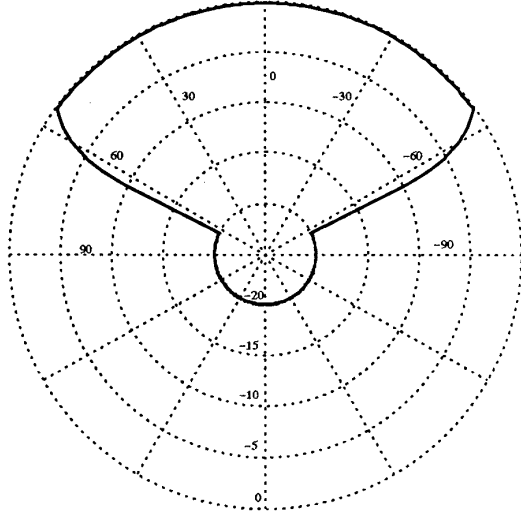


FIG. 4: Antenna characteristic model of sectorized antennas [dB]

ing and assuming that

$$P_{\text{received}} \sim P_{\text{transmitted}} \cdot d^{-\gamma}$$

([3], distance d between transmitter and receiver, propagation coefficient γ). The assumed antenna characteristic for the sectorized antennas is depicted in Fig. 4. It shows a constant gain of 0 dB in the forward direction, a rather steep transition within 10° on each side and a constant gain of -20 dB in the backward direction to model antenna sidelobes and reflections. The interference power is calculated with all interferers within a circle of radius $r = 9.7r_{\text{cell}}$ around an observed cell being active. So three rings of interferers are considered for the clusters $\langle 2 \times 3 \rangle$ and $\langle 3 \times 3 \rangle$, two for the $\langle 7 \rangle$ cluster and 2.5 for the $\langle 3 \times 4 \rangle$ cluster.

The evaluated C/I ratios for co-channel interference in the uplink and downlink are listed in Table 2 and Table 3. For the downlink we assumed equal transmit powers of all basestations. For the uplink ideal power control was performed, i.e. the received power at the nearest basestation is controlled to be constant. In both cases each mobile station is assumed to be at worst case position within a triangular kernel cell with the connected three base stations at its corners.

TABLE 2

Minimum co-channel C/I-ratio, downlink (in dB)

γ	architecture			
	$\langle 2 \times 3 \rangle$	$\langle 7 \rangle$	$\langle 3 \times 4 \rangle$	$\langle 3 \times 3 \rangle$
3.00	10.5	10.5	9.8	6.5
3.25	12.1	12.3	11.5	7.9
3.50	13.7	14.0	13.2	9.3
3.75	15.3	15.7	14.8	10.6
4.00	16.8	17.3	16.4	11.9

TABLE 3

Minimum co-channel C/I-ratio, uplink (in dB)

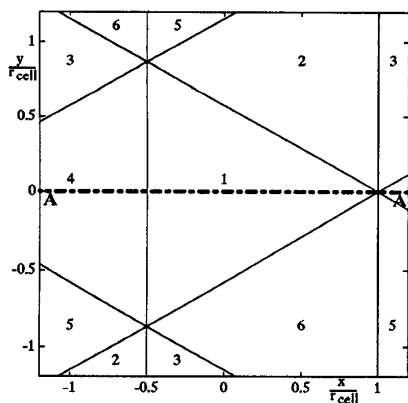
γ	architecture			
	$\langle 2 \times 3 \rangle$	$\langle 7 \rangle$	$\langle 3 \times 4 \rangle$	$\langle 3 \times 3 \rangle$
3.00	10.5	8.2	8.7	4.9
3.25	12.1	9.7	10.3	6.2
3.50	13.6	11.2	11.9	7.4
3.75	15.2	12.7	13.5	8.7
4.00	16.7	14.2	15.0	9.9

V. HANDOFF CONSIDERATIONS

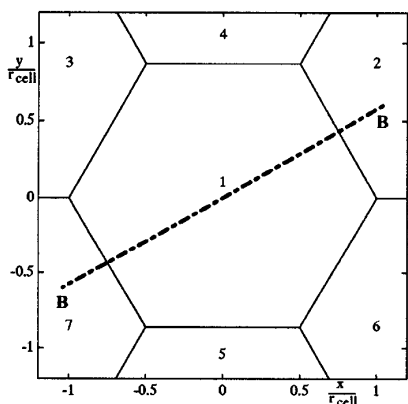
Since measurements of the received power performed by the mobile station are very important criteria for a handover decision, we have analyzed the characteristics of the new algorithm w. r. t. power differences and gradients. Fig. 5 shows the strongest carrier for the new architecture $\langle 2 \times 3 \rangle$ in comparison to the conventional $\langle 7 \rangle$ cluster with fading effects neglected. As expected, the dividing lines between areas with different carriers coincide with the ideal handoff lines.

As the field strengths of all used carriers along the line A-A of Fig. 5a show in Fig. 6a, the slopes of the received powers at both sides of the ideal handoff point -0.5 are very small, especially for the strongest carriers 1 and 4.

Within the conventional architecture $\langle 7 \rangle$ such problems do not occur because of larger gradients, as seen from Fig. 6b. Therefore one can conclude that the handoff decision within the new architecture should not be based on mobile station receiver power measurements only, but also on further information, e.g. on location information, since otherwise the advantages of the large handoff zones shown in Fig. 6 may not be utilizable.



(a) architecture $\langle 2 \times 3 \rangle$



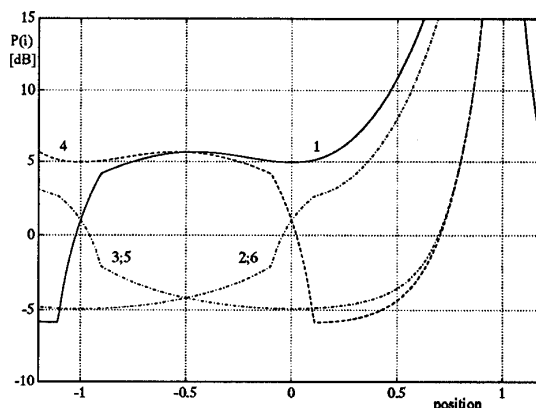
(b) architecture $\langle 7 \rangle$

FIG. 5: Best server areas

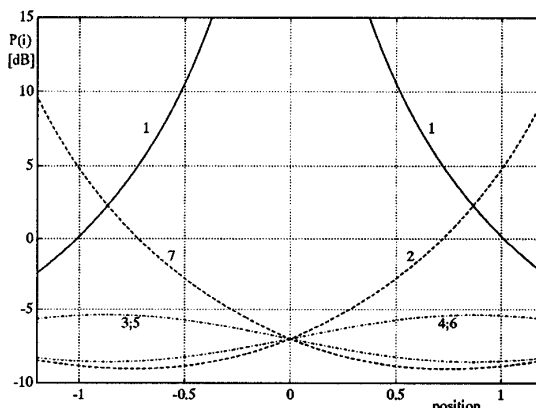
VI. PROPAGATION DELAYS

Multiple supply of the mobile station by three base stations results in different propagation delays, dependent on the actual location of the mobile station. Assuming ideal synchronization of the base stations, which means that there is no timing difference between the transmitted signals, the timing delay differences at the receiving point are depicted in Fig. 7 in multiples of a bit period ($= 3.69\mu s$, GSM system) per km cell radius.

The mobile station receiver has to cope with multipath propagation. Usually maximum-likelihood equalizers with 16 states are used in the GSM system corresponding to an equalization window of about $16\mu s$. The different propagation delays within the new cell architecture lead to a wider equivalent channel impulse response observed at



(a) architecture $\langle 2 \times 3 \rangle$, cross-section A-A



(b) architecture $\langle 7 \rangle$, cross-section B-B

FIG. 6: Received powers $P(i)$ of carriers i ($\gamma = 3.5$), cross-sections of cells in Fig. 5

the mobile station, namely the linear superposition of three single differently delayed channel im-

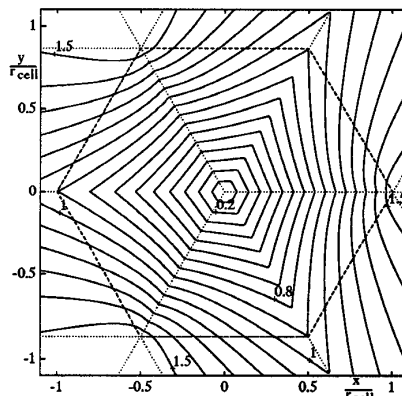


FIG. 7: Propagation delay differences (downlink) in bit periods (GSM) per km cell radius

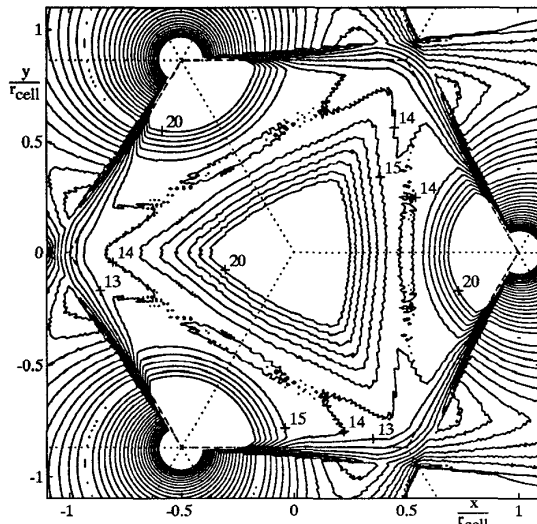


FIG. 8: Inherent C/I ratios [dB], channel profile *Typical Urban*, $\gamma = 3.5$, $r_{\text{cell}} = 4$ km

pulse responses. To measure the influence of this spreading, we calculated the inherent C/I-ratio to

$$\left(\frac{C}{I}\right)_i = \frac{\text{signal power inside equalization window}}{\text{signal power outside equalization window}}$$

Assuming a channel model *Typical Urban* as defined in GSM Recommendation 05.05 (for each of the three links) which is filtered by a gaussian shaped lowpass equivalent to GMSK modulation, we got inherent C/I rates for the whole cell area as depicted in Fig. 8 for a fixed cell radius of 4 km and a propagation coefficient $\gamma = 3.5$. The figure gives an idea of critical locations within a cell. The minimum C/I ratios within the cell area are presented in Table 4 as a function of the cell radius.

VII. CONCLUSIONS

The presented new system architecture shows excellent C/I ratios for the downlink as well as for the uplink, thereby allowing a re-use factor of 3. The system capacity is improved by a factor of 7/3 compared to a conventional cluster with a re-use factor of 7. As derived above, informations about the MS location should be available for an improved handoff decision. Due to multiple cell site supply, propagation delay differences cannot be neglected. Cell sizes are mainly restricted by the performance of the MS equalizer. For the

TABLE 4
Minimum inherent C/I ratio [dB] as in Fig. 8

r_{cell} [km]	γ				
	3.00	3.25	3.50	3.75	4.00
1.0	27.2	27.5	27.7	27.9	28.0
2.0	21.8	22.6	23.2	23.8	24.3
3.0	16.2	17.0	17.8	18.7	19.4
4.0	12.2	13.0	13.8	14.5	15.2
5.0	9.5	10.2	11.0	11.7	12.4
6.0	7.5	8.2	8.9	9.6	10.2

European GSM system, a maximum cell radius of about 4 km will be applicable.

VIII. ACKNOWLEDGMENT

We would like to thank the DETECON GmbH, Bonn, Germany, for supporting this work.

IX. REFERENCES

- [1] R. Bernhardt. Macroscopic diversity in frequency reuse radio systems. *IEEE Journal on Selected Areas in Communications*, 5(5):862–870, June 1987.
- [2] V. H. M. Donald. The cellular concept. *Bell System Technical Journal*, 58(1):15–41, Jan. 1979.
- [3] M. Hata. Empirical formula for propagation loss in land mobile radio services. *IEEE Transactions on Vehicular Technology*, 29(3):317–325, Aug. 1980.
- [4] W. C. Y. Lee. Spectrum efficiency in cellular. *IEEE Transactions on Vehicular Technology*, 38(2):69–75, May 1989.
- [5] W. C. Y. Lee. Smaller cells for greater performance. *IEEE Communications Magazine*, 29(11):19–23, Nov. 1991.
- [6] W. Papen, S. Zürbes, and W. Schmidt. Neue Netzarchitektur für den Mobilfunk mit Feststationen-Diversity und überlappenden Zellen. In *Aachener Kolloquium Signaltheorie: Mobile Kommunikationssysteme*, Berlin, March 1994. vde-verlag. (in German).